Cyanophosphine Derivatives: Nitrile or Cyanide Functionality?

Alexandrine Maraval,[†] Alain Igau,*[,†,‡] Christine Lepetit,[†] Anna Chrostowska,[§] Jean-Marc Sotiropoulos,[§] Geneviève Pfister-Guillouzo,*[,§] Bruno Donnadieu,[†] and Jean Pierre Majoral*[,†]

Laboratoire de Chimie de Coordination, CNRS, 205 route de Narbonne, 31077 Toulouse Cedex, France, and Laboratoire de Physico-Chimie Moléculaire, UMR 5624, Université de Pau & des Pays de l'Adour, Avenue de l'université, 64000 Pau, France

Received August 14, 2000

Treatment of dicyanophosphines $R-P(CN)_2$ with 1 equiv of Schwartz's reagent, $[Cp_2Zr(H)Cl]_n$, led: (i) via a substitution reaction to the formation of the stable hydrocyanophosphines R−P(H)CN (R = Me, ^{t}Bu, Mes*) or (ii) through a hydrozirconation reaction to the synthesis of the aldiminocyanophosphine $R-P(CH{=}NZrCp_2Cl)CN$ (R = N^{i}Pr$_2$). Further addition of 1 equiv of $[Cp_2Zr(H)Cl]_n$ to R−P(H)CN (R = Me, ^{t}Bu, Mes*) gave the primary phosphine $R-PH_2$ (R = Me) or the aldimino secondary phosphine $R-P(H)(CH{=}NZrCp_2Cl)$ (R = ^{t}Bu, Mes*) after the hydrozirconation reaction. Interestingly, the dialdiminophosphorus compound $R-P(CH{=}NZrCp_2Cl)_2$ (R = N^{i}Pr$_2$) was obtained after addition of $[Cp_2Zr(H)Cl]_n$ to $R-P(CH{=}NZrCp_2Cl)CN$ (R = N^{i}Pr$_2$). The difference in reactivity observed for the dicyanophosphines $R-P(CN)_2$ with the metal hydride $[Cp_2Zr(H)Cl]_n$ have been studied with the help of experimental analysis (UV−photoelectron spectroscopy, NMR, IR, X-ray) and computational methods.

Introduction

The chemistry of the cyano group has been extensively studied and used in organic, inorganic, and organometallic synthesis.[1] In the course of our studies, directed to the use of the interaction between main-group elements and group 4 elements for the development of new synthetic approaches for the synthesis of organic or inorganic species, we have been interested in the chemical behavior of cyanophosphines toward zirconocene complexes.[2] Very few studies have appeared on the coordination chemistry of dicyanophosphines, $R-P(CN)_2$.[3] We recently focused our attention on the study of the reactivity of dicyanophosphines $R-P(CN)_2$ with Schwartz's reagent $[Cp_2Zr(H)Cl]_n$ (**1**). Dicyanophosphines, $R-P(CN)_2$, may act on group 4 d^0 complexes,[4] Cp_2MXY (M = Ti, Zr), as triple-sided L type ligands which can coordinate to metal through both the P (soft) and N (hard) donor atoms (**A**). Moreover, our studies on the reactivity of mono(pseudo)halogenated derivatives R_2PX have shown that **1** could react as a

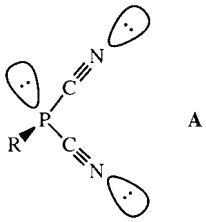

A

metal hydride reagent (X = Cl)[5] or the hydrozirconation reaction may be observed on the cyano group when X = CN.[6] It has long been established that changing substituents on phosphine derivatives can dramatically induce changes in the behavior of the free ligands and of their transition-metal complexes. This can be rationalized in terms of electronic and steric effects.[7] In a first approach, we will try to analyze with the help of experimental (photoelectronic spectra, molecular structure, IR and NMR spectroscopy) and computational evidence how these effects on dicyanophosphines, $R-P(CN)_2$, are responsible for the reaction observed and how one effect can dominate the other.

Results

Addition at −78 °C of 1 equiv of Schwartz's reagent $[Cp_2Zr(H)Cl]_n$ (**1**) to dichlorophosphine derivatives $R-PCl_2$ (**2a**−**e**) led to the formation of the corresponding primary phosphorus compounds $R-PH_2$ (**3a**−**e**) along with some remaining starting compound **2a**−**e** (Scheme 1). As expected, $[Cp_2Zr(H)Cl]_n$ (**1**) acts as a hydride

[†] Laboratoire de Chimie de Coordination, CNRS.
[‡] Fax: 05 61 55 30 03. E-mail: igau@lcc-toulouse.fr.
[§] Université de Pau & des Pays de l'Adour.

(1) *The Chemistry of the Cyano Group*; Patai, P., Series Ed., Rappoport, Z., Vol. Ed.; Wiley: London, 1970.

(2) Cadierno, V.; Donnadieu, B.; Igau, A.; Majoral, J. P. *Eur. J. Inorg. Chem.* **1999**, 417. Igau, A.; Dufour, N.; Straw, T.; Dewey, M.; Boutonnet, F.; Mahieu, A.; Zablocka, M.; Majoral J. P. *Phosphorus, Sulfur Silicon Relat. Elem.* **1993**, *77*, 283.

(3) (a) Nazmutdinova, V. N.; Chirkova, L. P.; Mukhamadeeva, R. M.; Plyamovatyi, A. Kh.; Gainullin, R. M.; Pudovik, M. A.; Polovnyak, V. K.; Pudovik, A. N. *Zh. Obshch. Khim.* **1994**, *64*, 1617. (b) Wilkie, C. A.; Parry, R. W. *Inorg. Chem.* **1980**, *19*, 1499. (c) Hoefler, M.; Schnitzler, M. *Chem. Ber.* **1974**, *107*, 194. (d) Sabherwal, I. H.; Burg, A. B. *Inorg. Chem.* **1972**, *11*, 3138. (e) Coskran, K. J.; Jones, C. E. *Inorg. Chem.* **1971**, *10*, 1664.

(4) Cardin, D. J.; Lappert, M. F.; Raston, C. L. *Chemistry of Organo-Zirconium and Hafnium Compounds*; Wiley: New York, 1986; and references therein.

(5) Zablocka, M.; Delest, B.; Igau, A.; Skowronska, A.; Majoral, J.-P. *Tetrahedron Lett.* **1997**, *38*, 5997.

(6) Boutonnet, F.; Dufour, N.; Straw, T.; Igau, A.; Majoral, J.-P. *Organometallics* **1991**, *10*, 3939.

(7) Tolman, C. A. *Chem. Rev.* **1977**, *77*, 313.

10.1021/om000704h CCC: $20.00
Publication on Web 12/09/2000

Scheme 1. Reactivity of R−PCl_2 (2a−e) with Schwartz's Reagent $[Cp_2Zr(H)Cl]_n$ (1)

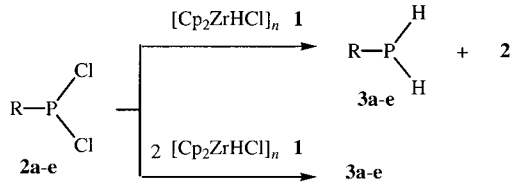

R= Me (**a**), ^{t}Bu (**b**), Mes* (**c**), Ph (**d**), N^{i}Pr$_2$ (**e**)

Scheme 2. Reactivity of R−$P(CN)_2$ (4a−e) with Schwartz's Reagent $[Cp_2Zr(H)Cl]_n$ (1)

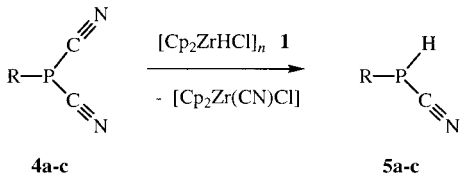

4a-c **5a-c**

R= Me (**a**), ^{t}Bu (**b**), Mes* (**c**)

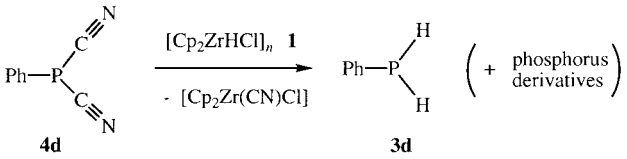

4d **3d**

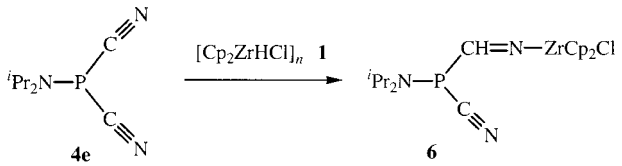

4e **6**

source[5] but no secondary halogenated phosphine R−P(H)-Cl was observed in the reaction mixture. Note that addition of 2 equiv of the metallocene complex **1** to **2** gave the phosphine **3** as the sole phosphorus product of the reaction.

In marked contrast with R−PCl_2 (**2a**−**c**) the corresponding dicyanophosphine compounds R−$P(CN)_2$ (**4a**−**c**) were reacted with 1 equiv of Schwartz's reagent **1** in toluene to give, after the loss of the metallic fragment $[Cp_2Zr(CN)Cl]$, the secondary cyanophosphine R−P(H)-CN (**5a**−**c**) in quantitative yield (Scheme 2). Compounds **5a**−**c** were unambiguously characterized by the usual spectroscopic methods. $^1J_{PH}$ coupling constants in the range of 210−250 Hz are characteristic for the P−H bond in phosphine compounds. Infrared spectroscopy ($\nu_{C\equiv N}$ = 1581−1583 cm^{-1}) and ^{13}C NMR ($\delta_{C\equiv N}$ = 119−122 ppm (d, $^1J_{CP}$ = 41−75 Hz)) corroborated the presence of the cyano PCN group in **5a**−**c**. Note that the reaction of **4d** with **1** does not give the expected primary phosphine PhP(H)CN. The behavior of **4d** is similar to that observed for **2d** with **1**; $PhPH_2$ was identified among other phosphorus derivatives.

Surprisingly, after 2 h in solution in toluene, the 1,2-addition of the Zr−H bond of **1** occurs on one of the two cyano groups in **4e** to give quantitatively the hydrozirconation reaction product **6** as one isomer (Scheme 2). The composition and constitution of **6** follow from mass analysis and ^{31}P, ^{1}H, and ^{13}C NMR spectra. The presence of the aldiminato moiety −CH=N− is proven by the significantly deshielded chemical shift in the ^{1}H NMR spectrum at δ_{CH} 9.34 ($^2J_{HP}$ = 75.4 Hz) ppm and in the ^{13}C NMR spectrum with the imino carbon at $\delta_{C=N}$ 171.8 ($^1J_{CP}$ = 17.0 Hz) ppm. The signal at 120.8 ($^1J_{CP}$ = 101.2 Hz) ppm can be attributed, as expected, to the nitrile carbon atom in cyano phosphine compounds.

Addition of 1 equiv of the Schwartz's reagent **1** to the secondary cyanophosphine **5a** led to a substitution reaction to give the corresponding primary phosphine $MePH_2$ ($\delta(^{31}P)$ −162 ($^1J_{HP}$ = 193 Hz) ppm) along with the loss of the metal fragment $[Cp_2Zr(CN)Cl]$ (Scheme 3). In marked contrast the secondary cyanophosphines **5b**,**c** reacted as nitrile compounds to give, after 1,2-addition of the zirconium−hydride bond to the C≡N group, the hydrozirconation products **7b**,**c** respectively, as one isomer (Scheme 3). The $^1J_{HP}$ coupling constants for **7b**,**c** of 213 and 234 Hz, respectively, are typical for a P−H bond in phosphine compounds. The chemical shift observed in ^{1}H NMR at 9.70 and 9.20 ppm for **7b**,**c** are characteristic for the aldimido CH=N protons. Cp groups of the metal fragment in the region of 6.00−6.20 ppm are inequivalent. At room temperature a 1,3-H sigmatropic rearrangement is observed for **7c**, giving the corresponding N-zirconated phosphaalkene product **8**. A COSY ^{1}H−^{1}H ^{31}P-decoupled experiment allows us to attribute a broad signal at 7.98 ppm to the NH group and at 8.01 ppm to the =CH fragment for **8**. Interestingly, the same products, **7b** and **8**, were obtained in a one-pot procedure starting from **4b**,**c** and 2 equiv of **1**. Note that the dihydrozirconated compound **9** is quantitatively prepared after addition of 1 equiv of **1** to **6**.[8] Only one isomer is identified. The ^{1}H NMR spectrum exhibited, besides the signals corresponding to the protons of the diisopropylamino groups, a doublet at 10.08 ($^2J_{HP}$ = 61.8 Hz) ppm, while the ^{13}C NMR spectrum displayed a doublet at 181.5 ($^1J_{CP}$ = 30.1 Hz) ppm characteristic of the aldimido groups HC=N.

Discussion

Phosphines of the type R−P(H)X with X = halogenated or pseudohalogenated groups are rare. These derivatives are normally unstable with respect to the loss of HX and consequent oligomerization to cyclophosphines, $(RP)_n$.[9,10] The stabilization of the phosphine unit R−P(H)X (X = Cl, Br, I) has been only accomplished with the use of very bulky groups (R = Mes*, $N(SiMe_3)_2$)[11] or with the strongly electronegative group (R = CF_3).[12] Note that no phosphine of the type R−P(H)CN has yet been isolated; only CF_3−P(H)CN was observed by ^{31}P NMR, but this decomposes by loss of HCN.[12] The hydridocyanophosphines R−P(H)CN (**5a**−**c**) are remarkably thermally stable toward α-elimination at the central phosphorus atom. Then, the study of the formation of these derivatives would be of interest with

(8) O'Neal, R. H.; Neilson, R. H. *Inorg. Chem.* **1984**, *23*, 1372 and references therein.

(9) Phosphines of the type R−P(H)X with X = F, Cl, Br, I stabilized as complex ligands are already known: Marinetti, A.; Mathey, F. *Organometallics* **1982**, *1*, 1488 and references therein.

(10) Cowley, A. H.; Kilduff, J. E.; Norman, N. C.; Pakulski, M. *J. Chem. Soc., Dalton Trans.* **1986**, 1801. Cowley, A. H.; Kilduff, J. E.; Lasch, J. G.; Norman, N. C.; Pakulski, M.; Ando, F.; Wright, T. C. *J. Am. Chem. Soc.* **1983**, *105*, 7751. Escudié, J.; Couret, C.; Ranaivonjatovo, H. J.; Satgé, J.; Jaud, J. *Phosphorus, Sulfur Relat. Elem.* **1983**, *17*, 221.

(11) Dobbie, R. C.; Gosling, P. D.; Straughan, B. P. *J. Chem. Soc., Dalton Trans.* **1975**, 2368.

(12) Maraval, A.; Donnadieu, B.; Igau, A.; Majoral, J. P. *Organometallics* **1999**, *18*, 3183.

Scheme 3. Reactivity of 5a−c and 6 with Schwartz's Reagent $[Cp_2Zr(H)Cl]_n$ (1)

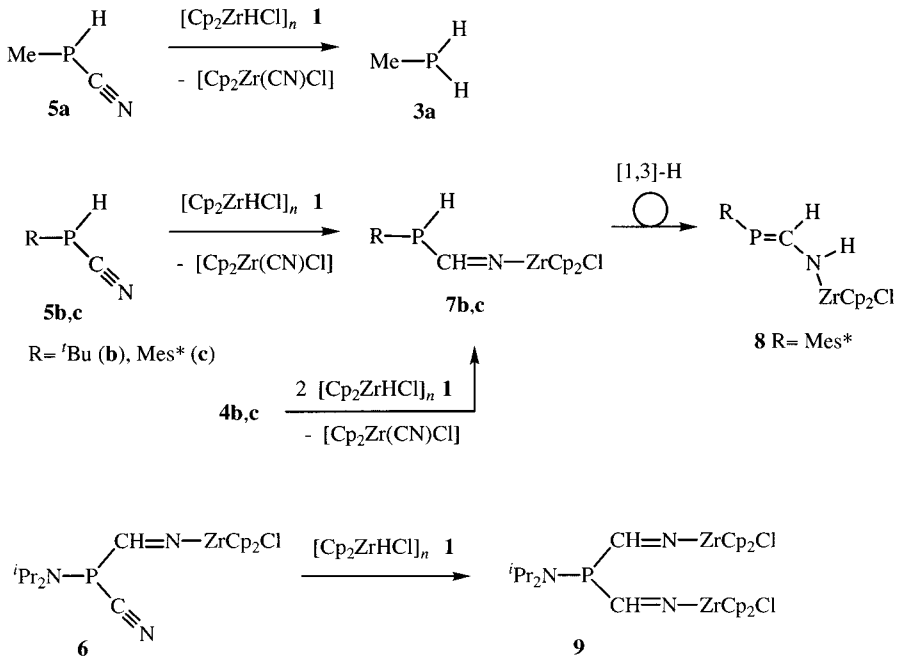

respect to the difference in reactivity observed between **4a**−**c** and **4e** with **1**.

Even if no experimental geometries are available for Schwartz's reagent **1**, theoretical studies and chemical evidence from the hydrozirconation reaction showed that a precoordination of the unsaturated molecule on the vacant site of the zirconocene(IV) metal fragment occurs in the transition states of the reaction process.[13] Phosphines and nitriles are good L type ligands in group 4 metallocene(IV) chemistry.[14] These two moieties are present in the structure of the cyanophosphines derivatives **4a**−**e**. Thus, three chelating centers are available for coordination on the vacant site of the zirconocene. The necessity of achieving good orbital overlap with the $1a_1$ orbital of zirconium implies coordination in the HZrCl plane; the angle between these three ligands cannot exceed 140°.[4] In a first approach, (i) a study of the electronic effect of the substituent R on the potentially chelating sites in **4a**−**e** using UV−photoelectron, NMR, and IR spectroscopy and (ii) an estimation of steric hindrance may help to understand the effect governing the chemical behavior of the dicyano compounds **4a**−**e** toward **1**.

The He I and He II photoelectron spectra of the series $R-P(CN)_2$ (**4a**−**e**) have been recorded and interpreted. The PE spectra assignment is based on the qualitative estimation of interactions between the cyano group, phosphorus lone pair, and substituent and have been compared with theoretical studies by the single-reference-based MP2 method,[15] in conjunction with the 6-311G(d,p) basis set, and the density functional theory (DFT)[16] with B3LYP[17] functional (Gaussian 98)[18] realized for **4a**,**e** and $Me_2N-P(CN)_2$. Qualitatively, we can consider the "through space " interaction in which the expected four $\pi^{\perp}_{CN}$ orbitals (b_2, a_2, b_1, and a_1) could be involved.[19] The presence of the phosphorus atom leads to an additional interaction with the b_1 orbital of the same symmetry. The calculated molecular orbital localization for **4a** (Figure 1) shows these interactions well. Considering this scheme, we can easily assign the photoelectron spectrum of **4a** (Figure 3a). The spectra of the phosphine **4a** gives rise to a first band at 10.8 eV, followed by one intense band at 12.7 eV and one larger band, centered at 13.5 eV. The first band can be assigned to the ejection of an electron of the phosphorus lone pair orbital; this attribution is confirmed by the decrease of the intensity using He II radiation. Note that there is an obvious stabilization to more than 1 eV relative to $Me-PH_2$ derivative. The integrated areas of the second band at 12.7 eV suggest that it may in fact be due to overlapping of the expected b_2, a_1, and a_2 ionizations. The intensity of the third band clearly increases compared to the two others, on going from He I to He II radiation, which corresponds well to the ionization of the n_N orbitals (b_2 and a_1). This broad band at 13.5 eV could also reasonably contain the ionization of the b_1 orbital.

Replacement of a Me group by a ^{t}Bu group causes a decrease in IP. The spectra of **4b** shows a first band at

(13) Endo, J.; Koga, N.; Morokuma, K. *Organometallics* **1993**, *12*, 2777.

(14) As an example see: Walsh, P. J.; Hollander, F. J.; Bergman, R. G. *J. Am. Chem. Soc.* **1990**, *112*, 894.

(15) Hehre, W. J.; Radom, L.; Schleyer, P. v. R.; Pople, J. A. *Ab Initio Molecular Orbital Theory*; Wiley: New York, 1986.

(16) Parr, R. G.; Yang, W. *Functional Theory of Atoms and Molecules*; Oxford University Press: New York, 1989.

(17) (a) Becke, A. D. *Phys. Rev.* **1988**, *38*, 3098. (b) Becke, A. D. *J. Chem. Phys.* **1993**, *98*, 5648. (c) Lee, C.; Yang, W.; Parr, R. G. *Phys. Rev.* **1988**, *B37*, 785.

(18) Frisch, M. J.; Trucks, G. W.; Schlegel, H. B.; Scuseria, G. E.; Robb, M. A.; Cheeseman, J. R.; Zakrzewski, V. G.; Montgomery, J. A., Jr.; Stratman, R. E.; Burant, J. C.; Dapprich, S.; Millam, J. M.; Daniels, A. D.; Kudin, K. N.; Strain, M. C.; Farkas, O.; Tomasi, J.; Barone, V.; Cossi, M.; Cammi, R.; Mennucci, B.; Pomelli, C.; Adamo, C.; Clifford, S.; Ochterski, J.; Petersson, G. A.; Ayala, P. Y.; Cui, Q.; Morokuma, K.; Malick, D. K.; Rabuck, A. D.; Raghavachari, K.; Foresman, J. B.; Cioslowski, J.; Ortiz, J. V.; Baboul, A. G.; Stefanov, B. B.; Liu, G.; Liashenko, A.; Piskorz, P.; Komaromi, I.; Gomperts, R.; Martin, R. L.; Fox, D. J.; Keith, T.; Al-Laham, M. A.; Peng, C. Y.; Nanayakkara, A.; Gonzalez, C.; Challacombe, M.; Gill, P. M. W.; Johnson, B.; Chen, W.; Wong, M. W.; Andres, J. L.; Head-Gordon, M.; Replogle, E. S.; Pople, J. A. *Gaussian 98*, revision A.7; Gaussian, Inc.: Pittsburgh, PA, 1998.

(19) Stafast, H.; Bock, H. *Z. Naturforsch.* **1973**, *28B*, 746−753.

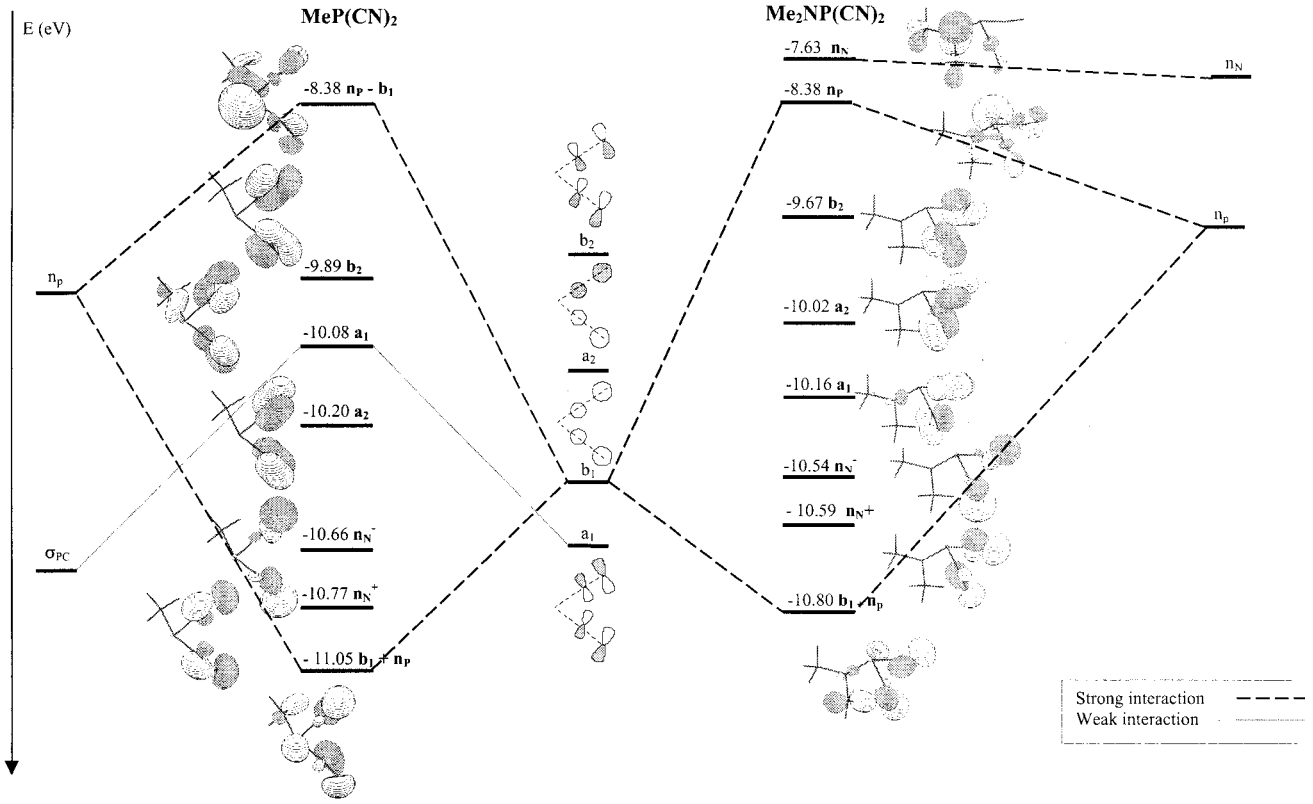

Figure 1. Correlation diagram resulting from "through space" and "through bond" interactions between the CN groups and the phosphorus and/or amino nitrogen lone pair orbitals for **4a** and $Me_2N-P(CN)_2$: B3LYP/6-311G** eigenvalues (in eV).

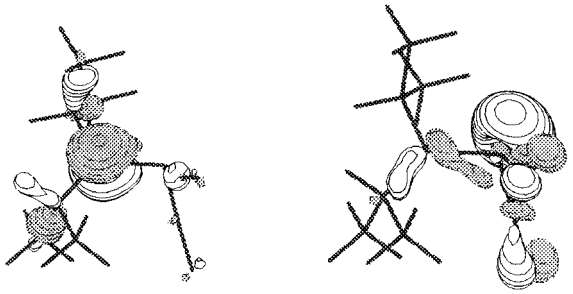

Figure 2. HOMO and HOMO-1 B3LYP/6-311G** for **4e**.

10.4 eV, always assigned to the ionization of the phosphorus lone pair, followed by four better resolved next bands, described as b_2 at 12.0 eV, a_1 at 12.5, a_2 at 12.8, and one more intense, at 13.3 eV corresponding to the n_N orbital ionizations and that of the b_1 orbital.

For the amino compound $R_2N-P(CN)_2$, a model compound of **4e** where the isopropyl substituents bonded to the nitrogen amino atom were replaced by methyl groups, $Me_2N-P(CN)_2$, was first considered. At the MP2 level, the calculated energetically privileged structure exhibits a slightly sp^3 nitrogen atom hybridization with a gauche lone pair orientation compared to the phosphorus one. The geometry of **4e** optimized at the B3LYP/6-311G** level exhibits an sp^2 nitrogen atom hybridization (sum of the valence angles 359.8°) in agreement with the geometry of the N^iPr_2 moiety generally observed in the Cambridge Data Base.[20] The orientation is also slightly gauche (around 5°). The position of the methyl substituents of the isopropyl group develops a difference between the cyano moieties. The interaction between the lone pairs is no longer visible. The HOMO is well localized on the nitrogen atom, whereas the phosphorus lone pair corresponds to HOMO-1 (Figure 2). The geometrical parameters of the calculated structures are described in Table 1 and show well that the nitrile groups are not equivalent in the calculated structure of **4e**.

Experimentally, the PE spectrum of **4e** (Figure 3e) shows two ionizations at 9.3 eV and at 10.35 eV followed by a broad massif at 12.5 eV and a band at 13.0 eV. The first bands are respectively assigned to the ejection of an electron from the amino nitrogen and the phosphorus lone pairs. The first orbital has a large localization on the nitrogen lone pair and the second on the phosphorus lone pair. The relative intensity variations in the He II spectrum demonstrate experimentally the presence at the same time of these combinations and the distinct participation. The massif at 12.2 eV contains, as expected, the b_2, a_2, and a_1 orbitals mixed with the same-symmetry CN orbital ionizations. Another clearly distinguishable band is the one at 13.0 eV; this intense peak can be assigned to the nitrogen atom lone pair orbitals from the cyano moieties.

In the case of **4c**,**d**, the spectra (Figure 3c,d) show a first ionization at 8.8 and 10.0 eV and a second band at 9.5 and 10.7 eV, respectively. Considering the rotation angle of the mesityl ring (vide infra), it seems reasonable to take into account a weak interaction between the aromatic ring and the phosphorus atom lone pair, but a more important one between the aromatic ring and the cyano groups. The broad shape of the first band,

(20) Hydrio, J.; Gouygou, M.; Dallemer, F.; Daran, J. C.; Balavoine, G. G. A. Private communication.

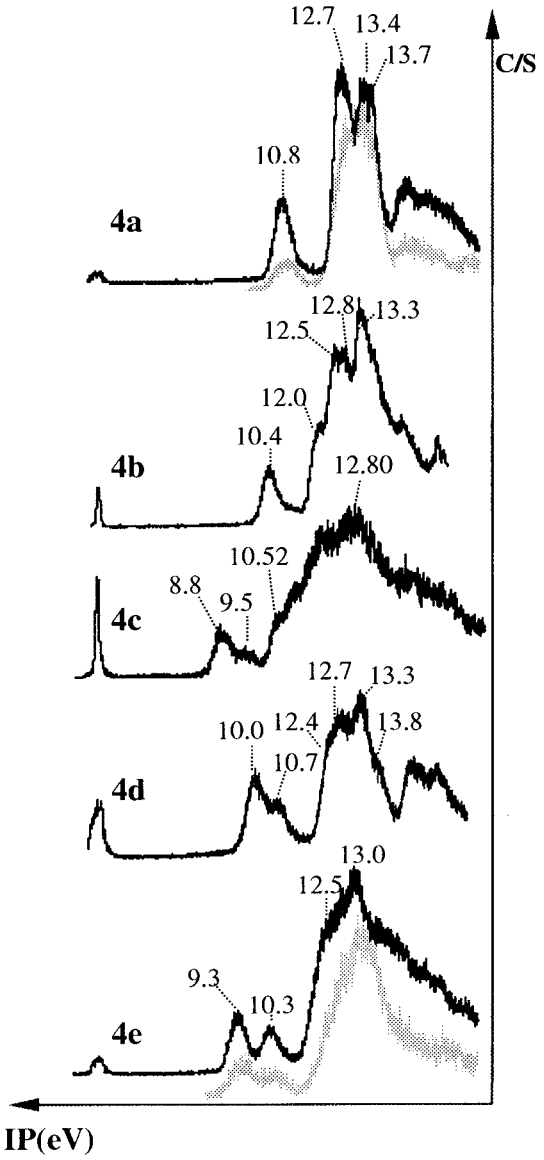

Figure 3. Photoelectron spectra of **4a**−**e**. For clarity, only He II spectra for the compounds **4a**,**e** are presented.

centered at 8.8 eV, is characteristic of the nondegenerated π_{aryl} system ionizations. The following band at 9.5 eV corresponds to the phosphorus atom lone pair orbital ionization. The same attribution can be proposed in the case of the phenyl derivative **4d**, in which the first band corresponds to the π_{phenyl} ionizations and the second band at 10.7 eV corresponds to the ejection of the electron localized on the phosphorus atom lone pair orbital.

In conclusion, the photoelectron spectra of **4a**−**e** show that the bands assigned to the phosphorus lone pair orbital ionization correspond to either the HOMO or the HOMO-1 and are in the range of 9.7 and 10.8 eV (Figure 4). Then, in comparison to the nitrile nitrogen lone pair, n_N (up to 14 eV), the phosphorus lone pair site, when accessible, can be reasonably envisaged as being coordinated on the metal fragment.

In comparison to **4e**, steric hindrance would be smaller for **4c**. However, this hypothesis cannot explain the behavior of **4c**,**e**. Another explanation can be found by considering the localization of the HOMO. The HOMO of an amino derivative such as **4e** shows a $\pi^{\perp}_{CN}$ orbital contribution (Figure 2), which could explain a precoordination on the CN system followed by the hydrozirconation reaction. However, due to the low localization on the π_{CN} orbitals, the latter reaction can be considered because of the reduced accessibility of the phosphorus lone pair.

Though this mechanism cannot be controlled by the charges, we have examined the repartition of the electronic population in order to estimate the characteristics of the P−substituent bond for **4a**−**e**.

The repartition of the electronic population in the dicyanophosphines **4a**−**e** have been examined with the help of the electron localization function (ELF).[21] According to our studies, no delocalization is observed from the lone pair of the phosphorus atom to the nitrile moiety for the dicyanophosphines **4a**−**e**. More surprisingly, the topological analysis of ELF provides a new description of the C−N chemical bond in nitrile compounds. According to the electronic population found for the C−N bond, the bond order is close to 2, whereas the electronic population of the nitrogen lone pair is larger than 3 (Table 5).[22] Indeed, the isosurface of the ELF is isotropic along the C−N axis and the analysis of the orbital contribution to the C−N bond shows that the π_X and π_Y systems have the same weight but are lower than two electrons. The picture given by AIM (topological analysis of the electron density within the theory of "atoms in molecules") is in agreement with the latter point, as the AIM charge resulting from integration of the population of the nitrogen core basin is close to about −1.4.[23] Then, as expected with the description given by ELF, the ellipticity, ϵ, which is a measure of the anisotropy of the electron density along the bond path in the AIM method, is found to be close to zero.[24] The comparison of the orbital contribution to the lone pair of N and P and of the P−C and C−N bonds is very similar for the methyl and ^{i}Pr$_2$N substituents. However, the nitrile groups are not completely equivalent in the case of the ^{i}Pr$_2$N substituent. Finally, in the case of the methyl substituent the contribution of the P−C's orbital to the electronic population of the phosphorus lone pair is about twice that obtained for the ^{i}Pr$_2$N substituent, suggesting that, in the case of an attack of Schwartz's reagent **1** at the phosphorus lone pair, the P−C bond would be strongly weakened in the case of the methyl substituent.

Photoelectron experiments and theoretical approaches point out the only interaction $b_1\pi_{CN}-n_P$. The cyano group ionizations remain well-distinguished, and the structure better corresponds to the resonance forms **I** and **II**, which is in full agreement with the IR and NMR analysis.

(21) Silvi, B.; Savin, A. *Nature* **1994**, *371*, 683. Savin, A.; Nesper, R.; Wengert, S.; Fässler, T. F. *Angew. Chem., Int. Ed. Engl.* **1997**, *36*, 1808.

(22) Note also that the bond order of the P−C bond is slightly greater than 1.

(23) Aray, Y.; Murgich, J.; Luna, M. A. *J. Am. Chem. Soc.* **1991**, *113*, 7135.

(24) Up to now, a value of zero found for ϵ was attributed to a single or a triple bond. It is important to note that, as expected, the picture derived from natural bond orbital analysis (NBO) is more classical (triple C−N bond ($\sigma + 2\pi$) and a nitrogen lone pair). Indeed, as mentioned by Bachrach (Bachrach, S. M. In *Reviews in Compututational Chemistry*; Lipkowitz, K. B., Boyds, D. B., Eds.; VCH: New York, 1994; pp 171−227), NBO rests on allocating electrons through an orbital occupancy basis, not in terms of the actual locations of electrons. The ELF analysis is expected to yield a more accurate picture of the molecule, as it takes into account the possible resonance forms, while NBO does not.

Table 1. Geometrical Parameters (Angles (deg), Bond Lengths (Å)) of 4a, $Me_2N-P(CN)_2$, and 4e[a]

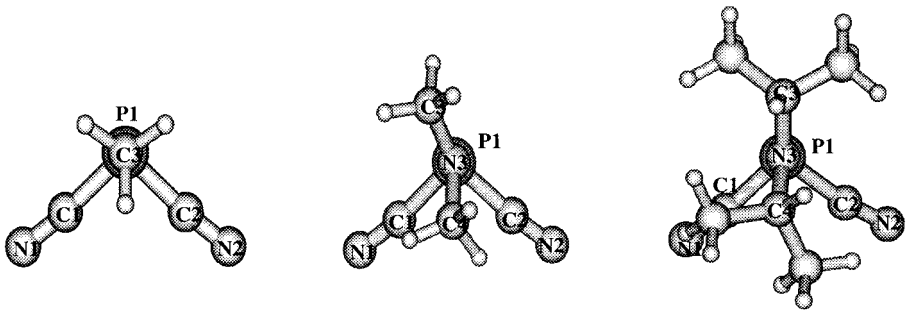

4a Me_2N-$P(CN)_2$ **4e**

4a			$Me_2N-P(CN)_2$			4e	
	MP2	B3LYP		MP2	B3LYP		B3LYP
P−C1	1.789	1.795	P−C1	1.793	1.803	P−C1	1.811
P−C2	1.789	1.795	P−C2	1.815	1.822	P−C2	1.806
C1−N1	1.179	1.156	C1−N1	1.179	1.156	C1−N1	1.157
C2−N2	1.179	1.156	C2−N2	1.181	1.157	C2−N2	1.157
P−C3	1.844	1.860	P−N3	1.689	1.684	P−N3	1.676
N1−C1−P	174.3	173.4	N1−C1−P	174.6	173.5	N1−C1−P	170.2
N2−C2−P	174.3	173.4	N2−C2−P	172.1	171.9	N2−C2−P	172.4
C1−P−C2	96.5	97.5	C1−P−C2	94.6	95.1	C1−P−C2	96.0
C1−P−C3	98.8	99.8	C1−P−N3	99.2	100.8	C1−P−N3	106.8
C2−P−C3	98.8	99.8	C2−P−N3	103.5	104.8	C2−P−N3	105.0
			P−N3−C3	114.5	116.8	P−N3−C3	115.9
			P−N3−C4	120.4	123.2	P−N3−C4	128.9
			C3−N3−C4	112.7	114.6	C3−N3−C4	115.0
			C4−N3−P−C1	−53.0	−52.4	C3−N3−P−C1	−59.0
			C4−N3−P−C2	44.0	45.9	C4−N3−P−C2	41.0

[a] Calculations were carried out at the 6-311G** level in all cases.

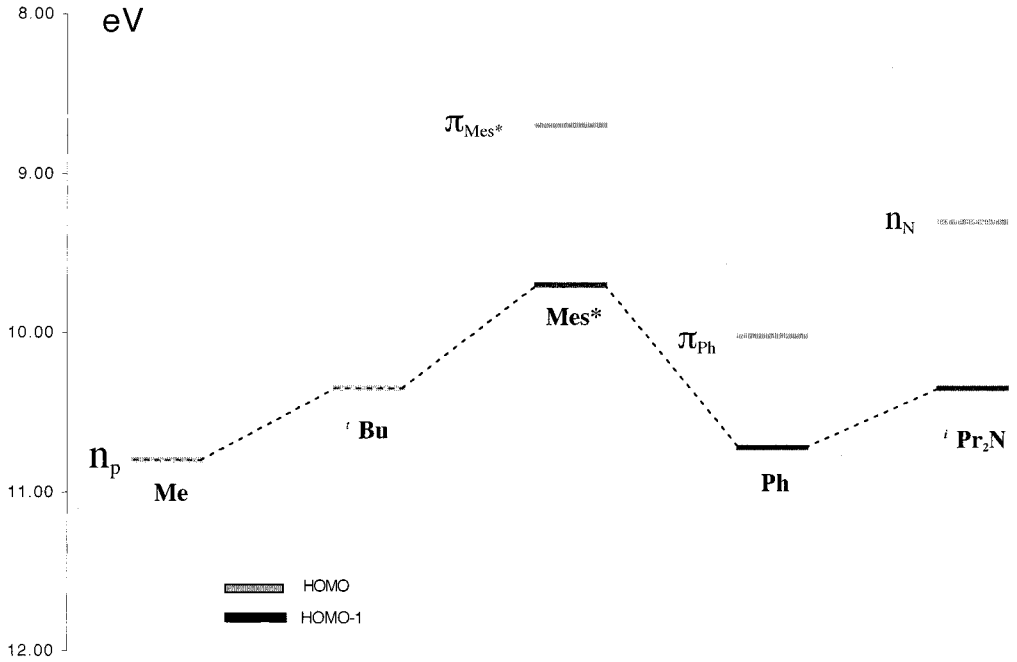

Figure 4. Ionization potentials (IP) of the compounds $R-P(CN)_2$ (**4a**−**e**).

In comparison to each other, the ^{31}P and ^{13}C NMR data for compounds **4a**−**e** do not exhibit any specific changes. The trend in the ^{31}P NMR chemical shift for dicyanophosphines **4a**−**e** follows the trend observed for the corresponding dihydro and dichloro phosphines RPX_2 (X = H, Cl).[25] The signal of the carbon atom in the P−C−N moiety of **4a**−**e** ($\delta(^{13}C)$ 113−119 ppm) is shifted to the region expected for organonitrile derivatives. In the infrared spectra the symmetric C−N stretching frequencies for compounds **4a**−**e**[26] appear in the close region of 2166−2182 cm^{-1}. Moreover, it is

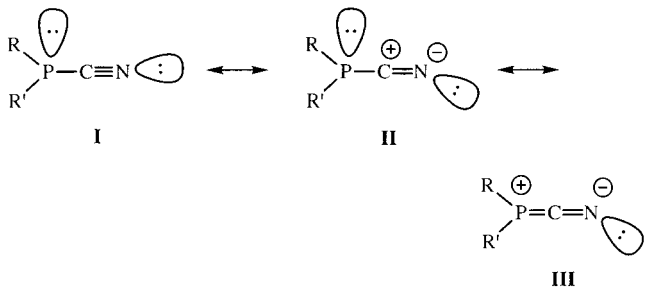

Table 2. Values of the Ligand Cone Angle θ

R=	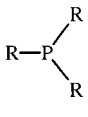	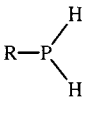	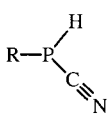	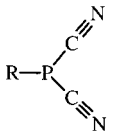
Me	118	97	108	116[b]
^{t}Bu	182	119	130	137[b]
Mes*	338	171	182	192[a]
Ph	145	101	117	128
^{i}Pr$_2$N	200	191	136	143[b]

[a] From the X-ray crystal structure. [b] Determined from the calculated structure with Cerius 2. Mes* = 2,4,6-^{t}Bu$_3$C$_6$H$_2$.

interesting to note that the symmetric C−N frequencies of Ph_2PCN, **4d**, and $Ph_2P(S)CN$ are in the same range and are equal to 2173, 2182, and 2180 cm^{-1}, respectively. Then NMR and IR spectroscopic data demonstrate that in the ground state dicyanophosphines **4a**−**e** do not exhibit heterocumulene character. This is in accord with what is observed with other phosphorus(III) compounds containing π-acceptor substituents, as for example CHO.[27] The structure of compounds **4a**−**e** is more in favor with resonance forms **I** and **II** rather than the cumulenic form **III**.

The steric accessibility of the lone pair of the phosphorus atom is also one of the factors which determines the coordination chemistry of the phosphine compounds. The steric hindrance of phosphines has been rationalized by Tolman in terms of the cone solid angle θ (Table 2).[7] In neutral zirconocene(IV) complexes, Cp_2ZrXY, phosphines are often used to stabilize the metal fragment. To the best of our knowledge, Ph_2PMe (θ = 136°) is the most hindered phosphine that has been coordinated to neutral zirconocene(IV) complexes.[28,29] Then, the significant degree of steric hindrance provided by the Mes* and the N^{i}Pr$_2$ groups should prevent any possible coordination of the lone pair of the phosphorus atom in **4c**,**e** on the zirconium fragment of **1**.

To gain more insight into the structure of the dicyanophosphine **4c**, X-ray crystallography was undertaken (Table 3, Figure 5). The bond distances and bond angles for **4c** are given in Table 4. The phosphorus is in a pyramidal environment (sum of the three bond angles 312°). The average P−CN bond length is 1.79 Å, and the average C−N bond is 1.14 Å. The bond angles at the phosphorus (C1−P1−C2) and at the carbon atoms of the cyano groups (P1−C1−N1 and P1−C2−N2) are 95.27, 171.3, and 168.5°, respectively. All these values are in good agreement with those observed for phosphorus tricyanide, $P(CN)_3$. The significant deviation

Table 3. Crystallographic Data, Summary of Data Collection, and Refinement Details for 4c

empirical formula	$C_{20}H_{29}N_2P$
fw	328.42
temp	160 (2) K
wavelength	0.710 73 Å
cryst syst, space group	monoclinic, *Cc*
unit cell dimens	a = 17.708(4) Å
	b = 9.518(2) Å
	c = 11.491(2) Å
	β = 95.92(3)°
V	1926.4(7) Å^3
Z, calcd density	4, 1.132 Mg/m^3
abs coeff	0.145 mm^{-1}
F(000)	712
cryst color	colorless
cryst form	parallelepiped
cryst size	0.8 × 0.6 × 0.4 mm^3
tube power	1.50 kW
tube voltage	50 kV
tube current	30 mA
collimator size	0.5 mm
detector dist	70.0 mm
2θ range	3.3−52.1°
d(hkl) range	12.453−0.809 Å
ψ movement mode	rotation
ψ start	0.0°
ψ end	250.5°
ψ increment	1.5°
no. of exposures	192
irradiation/exposure	5.00 min
index ranges	$-19 \le h \le 20$, $-11 \le k \le 11$,
	$-13 \le l \le 13$
no. of rflns collected/unique	6117/3072 (R(int) = 0.0638)
completeness to 2θ = 24.41	99.2%
refinement method	full-matrix least squares on F^2
no. of data/restraints/params	3072/2/217
goodness of fit on F^2	1.038
final R indices ($I > 2\sigma(I)$)	R1 = 0.0385, wR2 = 0.0953
R indices (all data)	R1 = 0.0415, wR2 = 0.0972
absolute structure param[37]	−0.05(8)
largest diff peak and hole	0.223, −0.182 e/Å^3

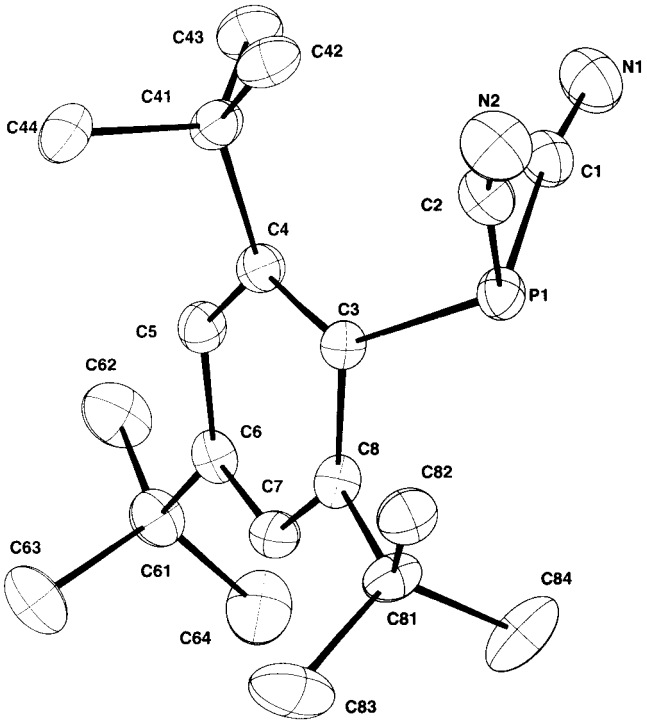

Figure 5. X-ray crystal structure of **4c** (ZORTEP drawing with thermal ellipsoids at 50% probability).

from linearity of the P−C−N linkage is surprising, and up to now there does not appear to be any ready explanation for it.[30] The most striking feature in the structure of compound **4c** is the position of the aryl group. The plane of the Mes* substituent deviates from the P−C3 bond axis by 33.4°. However, due to the steric hindrance of this bulky group, this deviation is com-

(25) It is well-established that cyanide shields the phosphorus atom, as does the hydrogen atom; there is an opposite effect for the chloro atom.[3b]

(26) The weak antisymmetric C−N stretching frequencies of **4a**−**e** have not been identified.

(27) Amsallem, D.; Gornitzka, H.; Baceiredo, A.; Bertrand, G. *Angew. Chem., Int. Ed.* **1999**, *38*, 2201.

(28) Cardin, D. J.; Lappert, M. F.; Raston, C. L. *Chemistry of Organozirconium and Hafnium Compounds*; Wiley: New York, 1986.

(29) Note that the cationic zirconocene complex $[Cp_2Zr(H)(Ph_2PMe)_2]^+$ has been characterized: Jordan, R. F.; Bajur, C. S.; Dasher, W. *Organometallics* **1987**, *6*, 1041.

Table 4. Selected Bond Distances (Å) and Angles (deg) for 4c

Distances			
P−C(1)	1.796(3)	P−C(2)	1.800(2)
P−C(3)	1.838(2)	C(1)−N(1)	1.142(3)
C(2)−N(2)	1.140(3)	C(3)−C(4)	1.413(3)
C(3)−C(8)	1.421(3)	C(4)−C(5)	1.388(3)
C(5)−C(6)	1.388(3)	C(6)−C(7)	1.394(3)
C(7)−C(8)	1.382(3)		
Angles			
P−C(1)−N(1)	171.2(2)	P−C(2)−N(2)	168.5(2)
C(1)−P−C(3)	102.42(10)	C(2)−P−C(3)	114.08(10)
C(1)−P−C(2)	95.24(12)	P−C(3)−C(4)	125.20(16)
P−C(3)−C(8)	110.97(14)		

Table 5. Average Populations (*N*) of Selected Basins Obtained from the Topological Analysis of ELF for 4a,c,e (See Scheme 2), MeP(O)(CN)$_2$, and MeCN

basin	model **4a**	model **4c**	model **4e**	MeP(O)(CN)$_2$	MeCN
V(P, CN)	2.4	2.4	2.4	2.4	2.1[a]
V(C,N)	4.3	4.3	4.2	4.3	4.5
V(P)	2.0	2.0	2.1		
V(N)	3.2	3.2	3.2	3.1	3.4

[a] V(C,CN).

monly observed as soon as a phosphorus atom of a phosphine is directly linked to the Mes* substituent.[31] These structural data confirm the presence of a weak interaction involving the phosphorus lone pair orbital and the sp^3 carbon C3 of the mesityl group.

Conclusion

We have found an easy way to prepare quantitatively the cyano primary phosphanes R−P(H)CN (**5a**−**c**) from the addition of Schwartz's reagent [Cp$_2$Zr(H)Cl]$_n$ (**1**) to the dicyanophosphine compounds R−P(CN)$_2$ (**4a**−**c**). Surprisingly, it is a hydrozirconation reaction which occurred on addition of **1** to ^{i}Pr$_2$N−P(CN)$_2$ (**4e**). Adding a further 1 equiv of **1** to **5a**−**c** gave the substitution product Me−PH$_2$ or the hydrozirconation products **7b**,**c**, respectively. Delineation of the factors—electronic and steric—that govern the reactivity of Schwartz's reagent **1** with dicyanophosphine derivatives R−P(CN)$_2$ (**4a**−**e**) is by no means straightforward. Nevertheless, experimental analysis (NMR, IR, UV−PES, X-ray) showed that, whatever the R group linked to the P(CN)$_2$ moiety, there is practically no interaction between the phosphorus lone pair and the cyano groups. In the photoelectron analysis the bands attributed to ionization of the phosphorus lone pair in **4a**−**e** correspond to either the highest occupied molecular orbital (HOMO) or HOMO-1. Then coordination of dicyanophosphine derivatives R−P(CN)$_2$ on the zirconium fragment by the lone pair of the phosphorus atom is largely expected for **4a**,**b**. However, for the phosphines **4c**,**e** coordination of the metal fragment should occur on the cyano groups, which results in the formation of completely different products with the metal hydride **1**, the hydrocyanophosphine **5c** and the aldimidophosphine **6**, respectively. In a first approach, one explanation can be found considering the molecular orbital, from the point of view of localization and accessibility. Apart from the steric effect, the HOMO of the amino derivative presents a $\pi^{\perp}_{CN}$ orbital contribution, which could explain a precoordination on the CN system followed by a hydrozirconation process. However, to rationalize the difference in reactivity of **4a**−**c** on one hand and **4e** on the other hand, a theoretical study of the reaction path seems to be required, especially of the first step yielding the intermediate resulting from the coordination of the dicyanophosphine to the metal center. The same theoretical investigations will be realized on hydrocyanophosphines **5a**−**c**, which exhibited a different chemical behavior with **1**.

It is interesting to note that the topological analysis of the electron localization function (ELF) in dicyanophosphine derivatives R−P(CN)$_2$ provides a new description of the chemical bond C−N in nitrile compounds. According to the electronic population found for the C−N fragment, the ELF analysis suggests that the resonance form P−C$^+$=N$^-$ has a strong weight (72%). This repartition of the electronic population in the CN does not depend on the group linked to the cyano moiety; the same electronic population is observed in the case of acetonitrile.

Experimental Section

All manipulations were performed under an argon atmosphere, either on a vacuum line using standard Schlenk techniques or in a Braun MB 200-G drybox. Solvents were freshly distilled from dark purple solutions of sodium/benzophenone ketyl (THF, toluene, benzene, diethyl ether), lithium aluminum hydride (pentane), or CaH$_2$ (CH$_2$Cl$_2$). Deuterated NMR solvents were treated with LiAlH$_4$ (C$_6$D$_6$, THF-d_8) or CaH$_2$ (CD$_2$Cl$_2$), distilled, and stored under argon. Nuclear magnetic resonance (NMR) spectra were recorded at 25 °C on Bruker MSL-400, AM-250, AC-200, and AC-80 Fourier transform spectrometers. Chemical shifts are given downfield relative to Me$_4$Si (^{1}H, ^{13}C) or H$_3$PO$_4$ (^{31}P), respectively. ^{13}C NMR assignments were confirmed by inverse gradient $\delta(^1H)-\delta(^{13}C)\{^1H,^{31}P\}$ HMQC and ^{31}P−^{1}H INEPT NMR experiments. Elemental and mass spectrum analyses obtained on a Nermag R10-10H were performed by the analytical service of the Laboratoire de Chimie de Coordination (LCC) of the CNRS. RPCl$_2$ (R = ^{t}Bu,[32] Mes*,[33] N^{i}Pr$_2$,[34] [Cp$_2$Zr(H)(Cl)]$_n$[35]) were prepared according to literature procedures. MePCl$_2$, PhPCl$_2$, AgCN, and Me$_3$SiCN were purchased from Aldrich and used without further purification.

Typical Procedure for the Preparation of Phosphinonitriles 4a and PhP(CN)$_2$. To a solution of **2a** (21.20 mmol) in CH$_3$CN (20 mL) at room temperature was added 2 equiv of AgCN (5.700 g; 42.50 mmol). The reaction mixture was stirred for 2.0 h at room temperature. The resulting suspension was filtered over Celite. The solvent was evaporated under vacuum.

Data for 4a. 4a was purified by sublimation (0.1 mmHg, 55 °C) to give a gray powder in 65% yield. Mp: 71 °C. ^{31}P{^{1}H} NMR (C$_6$D$_6$, 62.9 MHz): δ −81.1 ppm. ^{1}H NMR (C$_6$D$_6$, 200.1 MHz): δ 0.30 (d, $^2J_{HP}$ = 7.6 Hz, 3H, PCH$_3$) ppm. ^{13}C{^{1}H} NMR (C$_6$D$_6$, 62.9 MHz): δ 7.3 (d, $^1J_{CP}$ = 9.3 Hz, CH$_3$), 115.5 (d, $^1J_{CP}$ = 66.4 Hz, PCN) ppm. IR: γ(CN) 2179, 2060 cm^{-1}. Anal. Calcd for C$_3$H$_3$N$_2$P: C, 36.75; H, 3.08. Found: C, 36.62; H, 2.94.

(30) Emerson, K.; Britton, D. *Acta Crystallogr.* **1964**, *17*, 1134.
(31) Dubourg, A. Ph.D. Dissertation, Paul Sabatier University, Toulouse, France, 1990, No. 117A. Andrianarison, M.; Couret, C.; Declercq, J.-P.; Dubourg, A.; Escudié, J.; Ranaivonjatovo, H.; Satgé, J. *Organometallics* **1988**, *7*, 1545. Kandri-Rodi, A.; Declercq, J.-P.; Ranaivonjatovo, H.; Escudié, J. *Organometallics* **1995**, *14*, 1954.
(32) Voskuil, W.; Arens, J. F. *Recl. Trav. Chim. Pays-Bas* **1963**, *82*, 302.
(33) Cowley, A. H.; Norman, N. C.; Pakulski, M. *Inorg. Synth.* **1990**, *28*, 235.
(34) King, R. B.; Sadanani, N. D. *Synth. React. Inorg. Met.-Org. Chem.* **1985**, *15*, 149.
(35) Buchwald, S. L.; LaMaire, S. J.; Nielsen, R. B.; Watson, B. T.; King, S. M. *Tetrahedron Lett.* **1987**, *28*, 3895.

Data for $PhP(CN)_2$. $PhP(CN)_2$ was purified by distillation under reduced pressure (0.1 mmHg, 80 °C) to give a white solid in 78% yield. $^{31}P\{^1H\}$ NMR (C_6D_6, 62.9 MHz): δ −74.0 ppm. ^1H NMR (C_6D_6, 200.1 MHz): δ 6.79−7.37 (m, 5H, Ph) ppm. $^{13}C\{^1H\}$ NMR (C_6D_6, 62.9 MHz): δ 114.7 (d, $^1J_{CP}$ = 60.9 Hz, PCN), 130.4 (d, $^3J_{CP}$ = 10.1 Hz, *m*-Ph), 133.4 (s, *p*-Ph), 135.1 (d, $^2J_{CP}$ = 25.9 Hz, *o*-Ph) ppm. The *i*-Ph carbon atom was not identified. IR: γ(CN) 2184, 2092 cm^{-1}. Anal. Calcd for $C_8H_5N_2P$: C, 60.01; H, 3.15. Found: C, 59.78; H, 3.02.

Preparation of 4b. To a solution of **2b** (2.00 g, 12.6 mmol) in CH_2Cl_2 (10 mL) at room temperature was added 2 equiv of Me_3SiCN (2.50 g; 3.35 mL, 25.10 mmol). The reaction mixture was stirred for 4 days at room temperature. The volatiles were removed under vacuum. The residue was distilled under reduced pressure (5 mmHg, 92 °C) to give **4b** as a yellow oil in 83% yield. $^{31}P\{^1H\}$ NMR (C_6D_6, 62.9 MHz): δ −43.5 ppm. ^1H NMR (C_6D_6, 200.1 MHz): δ 0.85 (d, $^3J_{HP}$ = 17.5 Hz, 9H, CH_3) ppm. $^{13}C\{^1H\}$ NMR (C_6D_6, 62.9 MHz): δ 26.3 (d, $^2J_{CP}$ = 16.1 Hz, CH_3), 33.3 (d, $^1J_{CP}$ = 9.5 Hz, $C(CH_3)$), 113.4 (d, $^1J_{CP}$ = 68.5 Hz, PCN) ppm. IR: γ(CN) 2182 cm^{-1}. Anal. Calcd for $C_6H_9N_2P$: C, 51.43; H, 6.47. Found: C, 51.27; H, 6.39.

Preparation of 4c. To a solution of **2c** (2.50 g, 7.20 mmol) in CH_3CN (20 mL) at room temperature was added 2 equiv of Me_3SiCN (1.92 g; 1.92 mL, 14.40 mmol). The reaction mixture was stirred for 2 h at room temperature. The volatiles were removed under vacuum, and **4c** was obtained as a yellow powder in 87% yield. Mp: 92.3 °C. $^{31}P\{^1H\}$ NMR (CD_2Cl_2, 62.9 MHz): δ −80.6 ppm. ^1H NMR (CD_2Cl_2, 200.1 MHz): δ 1.34 (s, 9H, *p*-C(CH_3)), 1.67 (s, 18H, *o*-C(CH_3)), 7.59 (d, $^4J_{HP}$ = 4.2 Hz, 2H, CH_{Ar}) ppm. $^{13}C\{^1H\}$ NMR (CD_2Cl_2, 62.9 MHz): δ 32.5 (s, *p*-C(CH_3)), 35.5 (d, $^4J_{CP}$ = 5.8 Hz, *o*-C(CH_3)), 36.9 (d, $^3J_{CP}$ = 19.7 Hz, *o*-*C*(CH_3)), 41.6 (s, *p*-*C*(CH_3)), 118.9 (d, $^1J_{CP}$ = 69.1 Hz, PCN), 127.3 (d, $^3J_{CP}$ = 10.3 Hz, *m*-Ar), 157.8 (s, *p*-Ar), 162.3 (d, $^2J_{CP}$ = 18.9 Hz, *o*-Ar) ppm. IR: γ(CN) 2166 cm^{-1}. Anal. Calcd for $C_{20}H_{29}N_2P$: C, 73.14; H, 8.89. Found: C, 72.97; H, 8.85.

Preparation of 4e. To a solution of **2e** (4.30 g, 21.20 mmol) in CH_3CN (20 mL) at room temperature was added 2 equiv of AgCN (5.700 g; 42.50 mmol). The resulting solution was heated under reflux. After 3.5 h, AgCl was eliminated by filtration and the volatiles were removed under vacuum. **4e** was purified from the residue after distillation under reduced pressure (0.01 mmHg, 125 °C), leading to the final product as a white solid at room temperature in 86% yield. Mp: 34 °C. $^{31}P\{^1H\}$ NMR (C_6D_6, 62.9 MHz): δ −23.0 ppm. ^1H NMR (C_6D_6, 200.1 MHz): δ 0.71 (d, $^3J_{HH}$ = 6.7 Hz, 12H, CH_3), 3.09 (m, 2H, CHN) ppm. $^{13}C\{^1H\}$ NMR (C_6D_6, 62.9 MHz): δ 22.5 (s broad, CH_3), 52.6 (s broad, CHN), 117.7 (d, $^1J_{CP}$ = 69.7 Hz, PCN) ppm. IR: γ(CN) 2175 cm^{-1}. Anal. Calcd for $C_8H_{14}N_3P$: C, 52.45; H, 7.70. Found: C, 52.35; H, 7.58.

Preparation of 5a. A suspended solution of $[Cp_2Zr(H)(Cl)]_n$ (**1**; 0.395 g, 1.53 mmol) and **4a** (150 mg, 1.53 mmol) in CH_2Cl_2 (10 mL) was stirred for 1 h at 0 °C. **5a** and the solvent were transferred in a trap immersed in nitrogen liquid. The final product **5a** was used without further treatment. In an identical experiment in CD_2Cl_2, **5a** was identified by ^1H and ^{31}P NMR experiments as the sole product of the reaction. $^{31}P\{^1H\}$ NMR (CD_2Cl_2, 62.9 MHz): δ −119.9 ppm. ^1H NMR (CD_2Cl_2, 200.1 MHz): δ 1.47 (dd, $^2J_{HP}$ = 5.3 Hz, $^3J_{HH}$ = 7.9 Hz, 3H, CH_3), 4.15 (dq, $^1J_{HP}$ = 227.5 Hz, $^3J_{HH}$ = 7.9 Hz, 1H, PH) ppm. $^{13}C\{^1H\}$ NMR (CD_2Cl_2, 62.9 MHz): δ 1.6 (d, $^1J_{CP}$ = 8.0 Hz, PCH_3), 119.6 (d, $^1J_{CP}$ = 70.9 Hz, PCN) ppm.

Preparation of 5b. A suspended solution of $[Cp_2Zr(H)(Cl)]_n$ (**1**; 0.276 g, 1.07 mmol) and **4b** (150 mg, 1.07 mmol) in CH_2Cl_2 (8 mL) was stirred for 1 h at 0 °C. **5b** was isolated from the reaction mixture by trap-to-trap transfer and used without further treatment. $^{31}P\{^1H\}$ NMR (CD_2Cl_2, 62.9 MHz): δ −59.8 ppm. ^1H NMR (CD_2Cl_2, 200.1 MHz): δ 1.34 (d, $^3J_{HP}$ = 14.5 Hz, 9H, CH_3), 3.98 (d, $^1J_{HP}$ = 213.0 Hz, 1H, PH) ppm. $^{13}C\{^1H\}$ NMR (CD_2Cl_2, 62.9 MHz): δ 31.4 (d, $^2J_{CP}$ = 13.6 Hz, CH_3), 37.2 (d, $^1J_{CP}$ = 24.6 Hz, $C(CH_3)$), 121.4 (d, $^1J_{CP}$ = 41.0 Hz, PCN) ppm.

Preparation of 5c. A suspended solution of $[Cp_2Zr(H)(Cl)]_n$ (**1**; 0.118 g, 0.46 mmol) and **4c** (150 mg, 0.46 mmol) in toluene (10 mL) was stirred for one night at room temperature. The volatiles were removed in vacuo, and the product **5c** was extracted with pentane (2 × 20 mL) and isolated as an orange powder in 98% yield. $^{31}P\{^1H\}$ NMR (CD_2Cl_2, 62.9 MHz): δ −101.6 ppm. ^1H NMR (CD_2Cl_2, 200.1 MHz): δ 1.28 (s, 9H, *p*-CH_3), 1.57 (s, 9H, *o*-CH_3), 1.60 (s, 9H, *o*-CH_3), 5.95 (d, $^1J_{HP}$ = 249.7 Hz, 1H, PH), 7.51 (d, $^4J_{HP}$ = 2.8 Hz, 2H, CH_{aryl}) ppm. $^{13}C\{^1H\}$ NMR (CD_2Cl_2, 62.9 MHz): δ 30.7 (s, *p*-C(*C*H_3)), 32.4 (d, $^4J_{CP}$ = 6.5 Hz, *o*-C(*C*H_3)), 34.3 (s, *p*-*C*(CH_3)), 37.5 (s, *o*-*C*(CH_3)), 117.3 (d, $^1J_{CP}$ = 23.5 Hz, *i*-C_{aryl}), 121.2 (d, $^1J_{CP}$ = 74.4 Hz, PCN), 123.0 (d, $^3J_{CP}$ = 4.7 Hz, *m*-*C*H_{aryl}), 149.4 (s, *p*-C_{aryl}), 155.4 (s, *o*-C_{aryl}) ppm.

Reactivity of 4d with 1. A suspended solution of $[Cp_2Zr(H)Cl]_n$ (**1**; 0.241 g, 0.94 mmol) and **4d** (150 mg, 0.94 mmol) in CH_2Cl_2 (8 mL) was stirred for one night at room temperature to give $PhPH_2$ (^{31}P NMR (CH_2Cl_2, 62.9 MHz): δ −123.8 (t, $^1J_{HP}$ = 195.0 Hz, PH_2) ppm) and other unidentified phosphorus derivatives.

Preparation of 6. A suspended solution of $[Cp_2Zr(H)Cl]_n$ (0.282 g, 1.092 mmol) and **4e** (0.200 g, 1.092 mmol) in CH_2Cl_2 (8 mL) was stirred for 1 h at 0 °C. Removal of the solvent in vacuo of the clear brown reaction mixture gave **6** in nearly quantitative yield. $^{31}P\{^1H\}$ NMR (CD_2Cl_2, 62.9 MHz): δ 15.2 ppm. ^1H NMR (CD_2Cl_2, 200.1 MHz): δ 1.24 (d, $^3J_{HH}$ = 6.6 Hz, 6H, CH_3), 1.28 (d, $^3J_{HH}$ = 6.6 Hz, 6H, CH_3), 3.46 (sept d, $^3J_{HP}$ = 13.2 Hz, $^3J_{HH}$ = 6.6 Hz, 2H, CHNP), 6.17 (s, 5H, Cp), 6.26 (s, 5H, Cp), 9.34 (d, $^2J_{HP}$ = 75.4 Hz, 1H, CH=N) ppm. $^{13}C\{^1H\}$ NMR (CD_2Cl_2, 62.9 MHz): δ 23.2 (s, CH_3), 53.3 (s, CHNP), 110.7, 111.0 (s, Cp), 120.8 (d, $^1J_{CP}$ = 101.2 Hz, PCN), 171.8 (d, $^1J_{CP}$ = 17.0 Hz, C=N) ppm. IR (KBr, CH_2Cl_2): γ 2155 (C≡N), 1660 (CH=N) cm^{-1}.

Preparation of 7b. A suspended solution of $[Cp_2Zr(H)Cl]_n$ (0.224 g, 0.869 mmol) and **5b** (0.100 g, 0.869 mmol) in CH_2Cl_2 (10 mL) was stirred for 1 h at 0 °C. Removal of the solvent in vacuo of the brown reaction mixture gave **7b** in nearly quantitative yield. $^{31}P\{^1H\}$ NMR (CD_2Cl_2, 62.9 MHz): δ 3.3 ppm. ^1H NMR (CD_2Cl_2, 200.1 MHz): δ 1.33 (d, $^3J_{HP}$ = 10.6 Hz, 9H, CH_3), 3.61 (dd, $^1J_{HP}$ = 213.0 Hz, $^3J_{HH}$ = 4.8 Hz, 1H, PH), 6.14 (s, 5H, Cp), 6.31 (s, 5H, Cp), 9.70 (dd, $^2J_{HP}$ = 50.1 Hz, $^3J_{HH}$ = 4.8 Hz, 1H, CH=N) ppm. $^{13}C\{^1H\}$ NMR (CD_2Cl_2, 62.9 MHz): δ 29.9 (d, $^2J_{CP}$ = 10.6 Hz, CH_3), 31.6 (d, $^1J_{CP}$ = 10.8 Hz, $C(CH_3)$), 110.7 (s, Cp), 112.8 (s, Cp), 176.6 (d, $^1J_{CP}$ = 32.4 Hz, CH=N) ppm.

Preparation of 8. A suspended solution of $[Cp_2Zr(H)Cl]_n$ (0.127 g, 0.490 mmol) and **5c** (0.150 g, 0.490 mmol) in toluene (10 mL) was stirred at room temperature. ^{31}P and ^1H NMR showed the formation of **7c** along with the formation of **8**.

Data for 7c. ^{31}P NMR (CD_2Cl_2, 62.9 MHz): δ −44.0 (d, $^1J_{PH}$ = 233.9 Hz, PH) ppm. ^1H NMR (CD_2Cl_2, 200.1 MHz): δ 1.25 (s, 9H, *p*-CH_3), 1.55 (s, 9H, *o*-CH_3), 1.61 (s, 9H, *o*-CH_3), 5.45 (d, $^1J_{HP}$ = 233.9 Hz, 1H, PH), 6.04 (s, 5H, Cp), 6.20 (s, 5H, Cp), 7.48 (d, $^4J_{HP}$ = 1.6 Hz, 2H, CH_{aryl}), 9.20 (d, $^2J_{HP}$ = 37.6 Hz, 1H, CH=N) ppm. After 1 day at room temperature, **7c** was totally transformed into **8**. The volatiles were removed in vacuo, and the product **8** was extracted with pentane (2 × 20 mL) and isolated as an orange powder in 90% yield.

Data for 8. $^{31}P\{^1H\}$ NMR (CD_2Cl_2, 62.9 MHz): δ 95.5 ppm. ^1H NMR (CD_2Cl_2, 200.1 MHz): δ 1.27 (s, 9H, *p*-CH_3), 1.60 (s, 9H, *o*-CH_3), 1.63 (s, 9H, *o*-CH_3), 6.06 (s, 5H, Cp), 6.20 (s, 5H, Cp), 7.50 (d, $^4J_{HP}$ = 0.6 Hz, 2H, CH_{aryl}), 7.98 (dd, $^3J_{HH}$ = 16.5 Hz, $^3J_{HP}$ = 6.0 Hz, 1H, NH), 8.01 (dd, $^2J_{HP}$ = 49.7 Hz, $^3J_{HH}$ = 16.5 Hz, 1H, PCH) ppm. $^{13}C\{^1H\}$ NMR (CD_2Cl_2, 62.9 MHz): δ 31.6 (s, *p*-C(*C*H_3)), 32.5 (d, $^4J_{CP}$ = 6.9 Hz, *o*-C(*C*H_3)), 33.6 (s, *p*-*C*(CH_3)), 38.3 (s, *o*-*C*(CH_3)), 111.9 (s, Cp), 122.0 (s, *m*-*C*H_{aryl}), 133.2 (d, $^1J_{CP}$ = 58.7 Hz, *i*-C_{aryl}), 149.9 (s, *p*-C_{aryl}), 156.4 (s, *o*-C_{aryl}), 177.7 (d, $^1J_{CP}$ = 61.0 Hz, P=C) ppm.

Preparation of 9. A suspended solution of $[Cp_2Zr(H)(Cl)]_n$ (0.282 g, 1.092 mmol) and **6** (0.482 g, 1.092 mmol) in CH_2Cl_2 (10 mL) was stirred for 1 h at 0 °C. Removal of the solvent in vacuo of the clear brown reaction mixture gave **9** in nearly

quantitative yield. $^{31}P\{^1H\}$ NMR (C_6D_6, 62.9 MHz): δ 52.0. ^1H NMR (C_6D_6, 200.1 MHz): δ 1.43 (d, 12H, $^3J_{HH}$ = 6.6 Hz, CH_3), 3.42 (m, 2H, CHNP), 6.15, 6.10, 6.03, 5.96 (s, 5H, Cp), 10.08 (d, $^2J_{HP}$ = 61.8 Hz, 2H, CH=N) ppm. $^{13}C\{^1H\}$ NMR (CD_2Cl_2, 62.9 MHz): δ 24.0 (s, CH_3), 53.4 (s, CHNP), 110.5 (s, Cp), 181.5 (d, $^1J_{CP}$ = 30.1 Hz, CH=N). IR: γ(CH=N) 1647, 1624 cm^{-1}.

X-ray Analysis of 4c. Single crystals of **4c** were obtained in acetonitrile. X-ray diffraction analysis was carried out at 160 K on a STOE IPDS (imaging plate diffraction system) equipped with an Oxford Cryosystems cooler device. The crystal-to-detector distance was 70 mm with the crystal oscillated in φ. Crystal decay was monitored by measuring 200 reflections per image. The final unit cell was obtained by the least-squares refinement of 5000 reflections using Mo Kα radiation. (λ = 0.710 73 Å). The structure was solved by direct methods (SIR92[36]) and refined by least-squares procedures on F^2 (SHELXL97).[37] H atoms were located on a difference Fourier map, but they were introduced in calculations in idealized positions (d(C−H) = 0.96 Å), and their atomic coordinates were recalculated after each cycle of refinement. They were given isotropic thermal parameters 20% higher than those of the carbon to which they are connected. All non-hydrogen atoms were refined anisotropically, and in the last cycles of refinement a weighting scheme was used. The absolute configuration has been assigned on the basis of the refinement of the Flack parameter X,[38] which is sensitive to the polarity of the structure; the value of this parameter has been found to be close to zero (−0.05(8)), clearly indicating the correctness of the enantiomer choice. The drawing of the molecule was realized with ZORTEP[39] with thermal ellipsoids at the 50% probability level for non-hydrogen atoms. Further details on the crystal structure investigation are available on request from the Director of the Cambridge Crystallographic Data Centre, 12 Union Road, GB-Cambridge, U.K., on quoting the full journal citation.

Photoelectron Spectroscopy. The photoelectron spectra were recorded on a Helectros 0078 instrument, using a He I/He II source, equipped with a 127° cylindrical analyzer and monitored by a microcomputer supplemented with a digital analogic converter. The spectra were calibrated on the known autoionization of helium at 4.98 eV and nitrogen ionization at 15.59 eV.

Computational Details. Ab initio calculations were performed using Gaussian 98.[18] The optimization and vibrational analysis were carried out at a 6-311G(d,p) level of theory with inclusion of dynamic electron correlation at the MP2 level. Calculations were also realized using the density functional theory method,[15] using the exact exchange functional Becke 3LYP[16] with the basis set 6-311G(d,p). Equilibrium molecular geometries were fully optimized, and on the resulting geometry, second derivatives were calculated to find out if a minimum or a saddle point was obtained. Graphical representation of the nature of the molecular orbitals were obtained using a MOLDEN program.[40] Natural bond orbital analysis,[41] which represents ab initio molecular wave functions in terms of localized Lewis structures, was realized in order to provide a quantitative analytical framework for the interpretation of molecular orbitals interactions. ELF calculations and topological analysis were carried out with TopMoD.[42] Visualizations of ELF isosurfaces and basins were done with the freeware SciAn.[43]

Topological Analysis of ELF. The bonding in molecules may be investigated by different techniques. The topological methods investigate well-defined local functions. In the atoms in molecules theory of Bader, criteria are proposed in order to decide the existence and nature of the bonds from the electron density analysis. Two atoms are bound if a bond path may be found between them. The value of the Laplacian of the charge density at bond critical points allows one to discriminate between closed-shell and electron-shared (covalent) interactions. In the latter case, however, it is not possible to distinguish between the formation of an electron pair of opposite spin and the sharing of only one electron.

The same type of analysis may be performed using the electron localization function (ELF), but it will additionally allow measurement of the pairing of the electrons. ELF is defined as ELF = $1/[1 + (D_\sigma/D_\sigma^0)^2]$, in which D_σ and D_σ^0 are the excess local kinetic energies due to the Pauli repulsion (the difference of the kinetic energy of the actual Fermionic system with respect to the one of the bosonic system having the same density) for the actual system and for a homogeneous electron gas of the same density, respectively. ELF takes values between 0 and 1. When electrons are alone or form pairs of opposite spin, the Pauli principle has little influence, and the ELF is therefore close to 1. However, when parallel-spin electrons are close to one another, ELF comes close to 0.

The topological analysis of the ELF gradient field yields a partition of the molecular space in basins and attractors (i.e., the local maxima of ELF). The basins are classified into core, valence bonding, and nonbonding basins. A core basin contains the nuclei X (except for a proton) and will be referred to as C(X). A bonding basin lies between two or more core basins. Valence bonding basins are further distinguished, depending on their connectivity to the core basins. The topological analysis of the gradient field of ELF assigns a region of space—the basin—to each attractor, providing a partition of the molecular space analogous to that made in hydrography to define river basins and watersheds. Each valence basin is characterized by its synaptic order, which is the number of core basins with which it shares a common boundary. Therefore, the monosynaptic basins correspond to nonbonded pairs (referred to as V(X)), whereas the di- and polysynaptic basins are related to bi- and multicentric bonds (referred to as $V(X_1,X_2,X_3, ...)$. A localization domain is a space region limited by an iso-ELF surface. It has been shown that ELF performs partitions of the molecular space which are consistent with the Lewis description and with the VSEPR model.

Acknowledgment. This work was supported by the CNRS (France) and the Ministère de la Recherche et de l'Enseignement Supérieur (Ph.D. fellowship for A.M.). Acknowledgment is made to the institut du Développement de Ressources en Informatique Scientifique (IDRIS: Orsay, France), administrated by the CNRS, for the calculation facilities for this research and Dr. Gijs Schaftenaar for allowing us to use his graphical program Molden. We also thank Prof. B. Silvi for fruitful discussions.

Supporting Information Available: Tables giving atomic coordinates, bond lengths and angles, and anisotropic thermal parameters for **4c**. This material is available free of charge via the Internet at http://pubs.acs.org.

OM000704H

(36) Altomare, A.; Cascarano, G.; Giacovazzo, G.; Guargliardi, A.; Burla, M. C.; Polidori, G.; Camalli, M. SIR92: a Program for Automatic Solution of Crystal Structures by Direct Methods. *J. Appl. Crystallogr.* **1994**, *27*, 435.

(37) Sheldrick, G. M. SHELXL97: Program for the Refinement of Crystal Structures; University of Göttingen, Göttingen, Germany, 1997.

(38) Flack, H. *Acta Crystallogr.* **1983**, *A39*, 876.

(39) Zolnaï, L. ZORTEP: Graphical Program for X-ray Structure Analysis, University of Heidelberg, Heidelberg, Germany, 1998.

(40) See: http://www-srs.caos.kun.nl/~schaft/molden.

(41) (a) Reed, A. E.; Curtiss, L. A.; Weinhold, F. *Chem. Rev.* **1988**, *88*, 899. (b) Foster, J. P.; Weinhold, F. *J. Am. Chem. Soc.* **1980**, *102*, 7211.

(42) Noury, S.; Krokidis, X.; Fuster, F.; Silvi, B. TopMoD Package; Université Pierre et Marie Curie, 1997.

(43) Pepke, E.; Murray, J.; Lyons, J.; Hwu, T.-Y. SciAn; Supercomputer Research Institute of the Florida State University at Tallahassee, Tallahassee, FL, 1996.